The Meteoritical Society

Meteoritics & Planetary Science 45, Nr 10–11, 1638–1656 (2010)
doi: 10.1111/j.1945-5100.2010.01108.x

Asteroid 2008 TC_3—Almahata Sitta: A spectacular breccia containing many different ureilitic and chondritic lithologies

Addi BISCHOFF[1*], Marian HORSTMANN[1], Andreas PACK[2], Matthias LAUBENSTEIN[3], and Siegfried HABERER[4]

[1]Institut für Planetologie, Wilhelm-Klemm-Str. 10, 48149 Münster, Germany
[2]Geowissenschaftliches Zentrum, Universität Göttingen, Goldschmidtstrasse 1, 37077 Göttingen, Germany
[3]Laboratori Nazionali del Gran Sasso—I.N.F.N., S.S.17/bis, km 18 + 910, I-67010 Assergi (AQ), Italy
[4]Haberer-Meteorites, Ruhbankweg 15, 79111 Freiburg, Germany
[*]Corresponding author. E-mail: bischoa@uni-muenster.de

(Received 24 February 2010; revision accepted 11 August 2010)

Abstract–Asteroid 2008 TC_3 impacted Earth in northern Sudan on October 7, 2008. The meteorite named Almahata Sitta was classified as a polymict ureilite. In this study, 40 small pieces from different fragments collected in the Almahata Sitta strewn field were investigated and a large number of different lithologies were found. Some of these fragments are ureilitic in origin, whereas others are clearly chondritic. As all are relatively fresh (W0–W0/1) and as short-lived cosmogenic radioisotopes were detected within two of the chondritic fragments, there is strong evidence that most, if not all belong to the Almahata Sitta meteorite fall. The fragments can roughly be subdivided into achondritic (ureilitic; 23 samples) and chondritic lithologies (17 samples). Among the ureilitic rocks are at least 10 different lithologies. A similar number of different chondritic lithologies also exist. Most chondritic fragments belong to at least seven different E-chondrite rock types (EH3, EL3/4, EL6, EL breccias, several different types of EL and EH impact melt rocks and impact melt breccias; some of the latter are shock-darkened). In addition, two H-group ordinary chondrite lithologies were identified, and one sample of a chondrite type that is so far unique. The latter has some affinities to R chondrites. Oxygen isotope compositions of 14 fragments provide further fundamental information on the lithological heterogeneity of the Almahata Sitta meteorite. Based on the findings presented in this study, the reflectance spectrum of asteroid 2008 TC_3 has to be evaluated in a new light.

INTRODUCTION

Asteroid 2008 TC_3 was the first asteroid detected in space before impacting Earth and fell in the Nubian Desert of northern Sudan on October 7, 2008. Hundreds of mostly small fragments were recovered. The meteorite called Almahata Sitta was classified as a polymict ureilite (Jenniskens et al. 2009) based on the study of only one meteorite fragment from the strewn field. The analysis by these authors shows that this meteorite is "an achondrite, a polymict ureilite, anomalous in its class: ultra-fine-grained and porous, with large carbonaceous grains." We have studied 40 small pieces from different fragments collected in the Almahata Sitta strewn field and found a large number of different lithologies. Some of these fragments are ureilitic in origin, whereas others are clearly chondritic. As all are relatively fresh (W0–W0/1; see the Samples and Analytical Techniques section), there are strong indications that most, if not all belong to the Almahata Sitta meteorite fall.

In this study, we will present mineralogical and oxygen isotope data for several Almahata Sitta meteorite fragments and the results of a study of short-lived cosmogenic radioisotopes of two chondritic fragments. Some preliminary data have been published by Bischoff et al. (2010) and Horstmann and Bischoff (2010a).

SAMPLES AND ANALYTICAL TECHNIQUES

All 40 studied Almahata Sitta fragments were found as individual meteorite fragments of 2.6–50 g in the Almahata Sitta strewn field in two search campaigns about 9 and 12 months after the meteorite fall. Most samples have a complete black to dark-brownish fusion crust. The partly brownish taint of several samples (e.g., MS-CH, MS-16, MS-152, and MS-165) is certainly the effect of desert weathering that occurred between the fall and the recovery. As all samples contain significant abundances of metal, the weathering grade in their interior can easily be determined. Based on Wlotzka (1993), no sample has a weathering degree higher than W0/1 as indicated by a slight brownish taint in transmitted light and/or by only very thin rinds of weathering products surrounding the metal grains (Tables 1 and 2). This fresh appearance is well-documented for 12 of the 40 samples in Figs. 1–5, where metals are shown in reflected light or backscattered electron (BSE) images.

A small piece of each of these fragments was selected for thin section preparation. Two sliced or partly sliced fragments of 5.1 g (MS-CH) and 8.65 g (MS-D) were used to measure the short-lived nuclides at the Laboratori Nazionali del Gran Sasso (LNGS, Italy; Tables 3 and 4). Small grains from several different fragments (<5 mg each) were prepared for oxygen isotope measurements at the Universität Göttingen (Germany).

The mineralogy and texture of the fragments were studied by light and electron optical microscopy. A JEOL 6610-LV electron microscope was used to resolve the fine-grained textures and to analyze the mineral constituents using the EDS attached (INCA; Oxford Instruments). As natural standards we used olivine (Mg, Fe, Si), jadeite (Na), plagioclase (Al), sanidine (K), diopside (Ca), rutile (Ti), chromite (Cr), rhodonite (Mn), and pentlandite (Ni).

The oxygen isotope compositions of 14 fragments were measured by laser fluorination gas mass spectrometry. Sample material (typically ~1–2 mg) is reacted with purified F_2 gas with aid of a 50 W infrared laser. Excess F_2 is reacted to Cl_2 in a NaCl trap and Cl_2 is trapped in a cold trap (−196 °C). Sample O_2 is analyzed in continuous flow mode with a ThermoElectron MAT 253 gas mass spectrometer. Accuracy and precision in $\delta^{18}O$ and $\Delta^{17}O$ are typically $\pm 0.2‰$ and $\pm 0.06‰$, respectively. The terrestrial fractionation line (TFL) is defined by 290 analyses of rocks and minerals to $\beta = 0.5250 \pm 0.0007\,(1\sigma)$.

The short-lived cosmogenic radioisotopes of two chondritic fragments from the Almahata Sitta strewn field were measured by means of gamma ray spectroscopy. The measurements were performed using high-purity germanium (HPGe) detectors, in ultra-low-background configuration (25 cm of lead and an inner liner of 5 cm copper, inside an underground laboratory with 1400 m rock overburden). The counting efficiency was determined with a thoroughly tested Monte Carlo code. The samples were measured from October 13 to 18, 2009 in the case of the sample MS-CH, and from November 9 to December 6, 2009, in the case of the sample MS-D.

RESULTS

In this study, we will present mineralogical and oxygen isotope data, as well as the results of a cosmogenic radioisotope study on various meteorite fragments from the Almahata Sitta strewn field. The fragments can roughly be subdivided into achondritic (ureilitic; 23 samples) and chondritic lithologies (17 samples). Main mineralogical characteristics are given in Tables 1 and 2. Details on some fragments have been previously presented by Bischoff et al. (2010) and Horstmann and Bischoff (2010a). Please note that the statistics of different lithological objects presented in Tables 1 and 2 may not be representative for the real distribution of collected fragments.

Mineralogy—Ureilitic Lithologies

Ureilites constitute the second largest group of achondritic meteorites next to the howardites, eucrites, and diogenites (HEDs). The majority (~77%; Mittlefehldt et al. 1998) of the unpaired monomict ureilites consist of olivine and pigeonite as major phases and contain interstitial carbon (up to ~5 vol%) as graphite or diamond, with minor abundances of other phases. Olivine compositions span a large range, from Fo approximately 75 to 95. In some, the pyroxene is augite and/or orthopyroxene instead of pigeonite. In addition, approximately 10% of the ureilites are polymict breccias, containing a few percent of feldspathic material in addition to typical ureilitic components, as well as exotic clasts (Mittlefehldt et al. 1998; Goodrich et al. 2004). One dimict ureilitic breccia is also known (Goodrich et al. 2004). Accessory interstitial phases of ureilites include metal, sulfides, and minor fine-grained silicates. Plagioclase is absent in monomict ureilites (e.g., Mittlefehldt et al. 1998; Goodrich et al. 2004). The formation of ureilites is highly controversial. Some authors suggest that the large range of observed olivine compositions is due to various degrees of carbon redox controlled reduction (smelting) of a common precursor material (e.g., Berkley and Jones 1982; Warren and Kallemeyn 1992;

Table 1. Ureilitic lithologies in the Almahata Sitta meteorite.

Fragment no.	Fragment mass (g)	Found	Shock[a]	W[b]	Typical grain size[c]	Ol cores (Fa)	Range (Fa)	Px cores (Fs)	Range (Fs)	Px cores (Wo)	Comments
Coarse-grained ureilitic fragments											
MS-16	4.31	7/2009	S3	W0/1	500–800 μm	5–6	2–6	5–6	5–6	3–4.5	Px-dominating; 4–5 wt% Ni in metal; ureilitic?
MS-153	7.43	7/2009	S2	W0/1	100–300 μm	10–12	8–13	10–11.5	3.5–11.5	4–5	Pyroxene-rich
MS-156	16.00	7/2009	S2	W0	> 1 mm	17–19	4–19	11–12.5	4–12.5	1–8	
MS-157	3.68	7/2009	S2	W0/1	0.8–1.2 mm	12–13	2–13	10–11	2–11	4.5–5	
MS-160	8.39	7/2009	S3	W0	> 1 mm	17–19	1–19				Pyroxene-poor
MS-162	4.74	7/2009	S3	W0/1	400–600 μm	16–18	1.5–18	6–7	2–7	4–4.5	Grains up to 2.5 mm
MS-167	49.14	10/2009	S3	W0/1	0.6–1.5 mm	20.5–22	2–22	17–18.5	1–18.5	11–11.5	
MS-169	26.29	10/2009	S3	W0	300–600 μm	11–12.5	1–12.5	10.5–11	0.5–11	5–9	Pyroxene-rich
MS-170	26.81	10/2009	S3	W0/1	400–800 μm	20–22	1–22	17–19	3–19	6–7	
MS-171	34.35	10/2009	S2	W0	100–300 μm	15–16.5	5–16.5	12–14	9–14	2–9	Variable grain size
MS-173	32.30	10/2009	S3	W0/1	0.8–1.2 mm	11.5–13.5	6–13.5	10.5–11.5	0.5–11.5	4.5–5.5	Pyroxene-rich
MS-175	7.46	7/2009	S2	W0/1	300–600 μm	10–12	2–12	8–10	2–10	4.5–5	Pyroxene-rich
Fine-grained ureilitic fragments											
MS-20	3.55	7/2009	recry. Ol	W0/1	< 30 μm	8–9	0–9	12–15	0–15	1.5–8	Metal-rich areas with niningerite
MS-28	37.92	7/2009	recry. Ol	W0/1	< 20 μm	11–13	3–13	13–16	2–16	2–6.5	
MS-61	16.55	7/2009	recry. Ol	W0/1	< 20 μm	Mainly: 14–16	2–19	14–17	3–17	3.5–7	Cores in some areas $Fa_{18–19}$
MS-124	34.02	7/2009	recry. Ol	W0/1	Mostly: < 20 μm	19–21	3–21	16–18	1–18	3–10	Contains coarser-grained fragment
MS-152	9.13	7/2009	recry. Ol	W0/1	< 30 μm	18–21	2–21	14–16	7–16	3.5–6	Reduced fragment: $\sim Fa_1$
MS-154	4.18	7/2009	recry. Ol	W0/1	< 20 μm	11–14	0–14	6–8	1.5–8	1–10	Areas with olivine cores of $\sim Fa_{<5}$ dominate
MS-161	4.88	7/2009	recry. Ol	W0/1	< 30 μm	18–19.5	1–19.5	14.5–15.5	12–15.5	3.5–9	Suessite
MS-165	2.63	7/2009	recry. Ol	W0/1	< 20 μm	15–18	2.5–18	12–14	0–14	3–6	Area with niningerite
MS-168	33.18	10/2009	recry. Ol	W0/1	< 20 μm	Mainly: 8–11	0–21	8–14	0–14	1.5–4	Areas with 18–20.5 mole% Fa and $Fa_{<5}$ occur
Metal–sulfide dominated fragments with enclosed ureilitic portions											
MS-158	9.05	7/2009	recry. Ol	W0/1	< 20 μm	17–20	10–20	Not analyzed			Data for the fine-grained portion
MS-166	3.25	7/2009	recry. Ol	W0/1	Up to 120 μm	12–14	2–14	13–16	2–15	2–9	Coarse-grained Ol inclusion; Ni-rich metals

Note: W = weathering; Ol = olivine; Px = low-Ca pyroxene; recry. Ol = recrystallized olivine.
[a]Shock metamorphism determined based on the classification schemes for ordinary and enstatite chondrites by Stöffler et al. (1991) and Rubin et al. (1997).
[b]Weathering grade W0/1 (Wlotzka 1993) assigned based on the slight brownish taint in restricted areas of the thin section as observed in transmitted light.
[c]For the coarse-grained ureilitic fragments, the grain size determination can only be a rough estimate, because of the limited sample size. In some cases, only a few grains were available.

Table 2. Chondritic lithologies in the Almahata Sitta meteorite.

Fragment no.	Fragment mass (g)	Found	Class	Shock[a]	W[b]	Fa	Fs	Fs (range)	Sulfides	Ni in metal (wt%)	Si in metal (wt%)	Comments
MS-D	17.34	7/2009	EL6	S2	W0/1		< 0.3		Oldhamite, troilite, keilite, Zn-alabandite	5.5	0.9	Breccia
MS-CH	5.68	7/2009	Unique	S2	W0/1	Mainly: 35–37	14.4 ± 7.5	3–26	Troilite	Mainly: ~38; Co: ~2	< 0.2	Fa range: 19–38; matrix: ~40 vol%
MS-7	8.73	7/2009	EL5/6	S2	W0/1		< 0.3		Oldhamite, troilite, keilite	6.9	0.8	Breccia?
MS-11	6.88	7/2009	H5/6	S3	W0/1	16.5	14		Troilite	7.6	< 0.2	Co in metal: ~0.8; shock-melted areas
MS-13	5.02	7/2009	EH IMR	S3	W0/1		0.6 ± 0.4	0–1.6	Oldhamite, troilite, niningerite, keilite	5.5	2.7	Shock-darkened
MS-14	4.69	7/2009	EH3	S3	W0/1		2.9 ± 3.7	0–13	Oldhamite, troilite, daubreelite, niningerite	4.2 (3.2–6.5)	3.1	Perryite
MS-17	4.22	7/2009	EL3/4	S2	W0/1	0.2 (1 grain)	0.5 ± 0.3	0–1	Oldhamite, (Zn-)alabandite, troilite, keilite	6.3	0.5	Contains shock-melted areas
MS-52	18.17	7/2009	EL6	S2	W0/1		< 0.3		Troilite, oldhamite, alabandite	6.4	0.9	
MS-79	14.71	7/2009	EL6	S2	W0		< 0.4		Troilite, oldhamite, alabandite	6.4	0.9	
MS-150	25.46	7/2009	EL IMR	S2	W0/1		< 0.3		Oldhamite, troilite, keilite	6.3	1.5	Schreibersite
MS-151	4.78	7/2009	H5	S2	W0/1	20.5	17.5		Troilite	8.2	< 0.1	Co in metal: ~0.7; shock-darkened
MS-155	3.11	7/2009	EH IMR	S3	W0/1		0.38 ± 0.2		Oldhamite, troilite, niningerite, keilite	5.6	3.3	Shock-darkened
MS-159	4.23	7/2009	EL IMR	S2	W0/1		0.4 ± 0.3		Oldhamite, troilite, keilite, one grain of niningerite	5.6	0.8	Breccia; niningerite-bearing (EH) fragment?
MS-163	9.94	7/2009	EH IMR	S2	W0/1		1.1 ± 0.55	0.1–1.9	Troilite, keilite, niningerite, oldhamite	6.5	3.3	Shock-darkened
MS-164	8.90	7/2009	EL3/4	S2	W0		0.4 ± 0.5	0–2	Oldhamite, troilite	5.6	1.4	Schreibersite, contains shock-melted areas
MS-172	45.52	10/2009	EL IMR	S2	W0/1		< 0.3		Troilite, keilite, oldhamite, alabandite	6.5	1.2	
MS-174	12.24	7/2009	EL6	S2	W0/1		< 0.3		Troilite, oldhamite, alabandite, keilite	6.3	0.8	Breccia

Note: IMR = impact melt rock; W = weathering.
[a]Shock metamorphism determined based on the classification schemes for ordinary and enstatite chondrites by Stöffler et al. (1991) and Rubin et al. (1997).
[b]Weathering grade W0/1 (Wlotzka 1993) assigned based on the slight brownish taint in restricted areas of the thin section as observed in transmitted light.

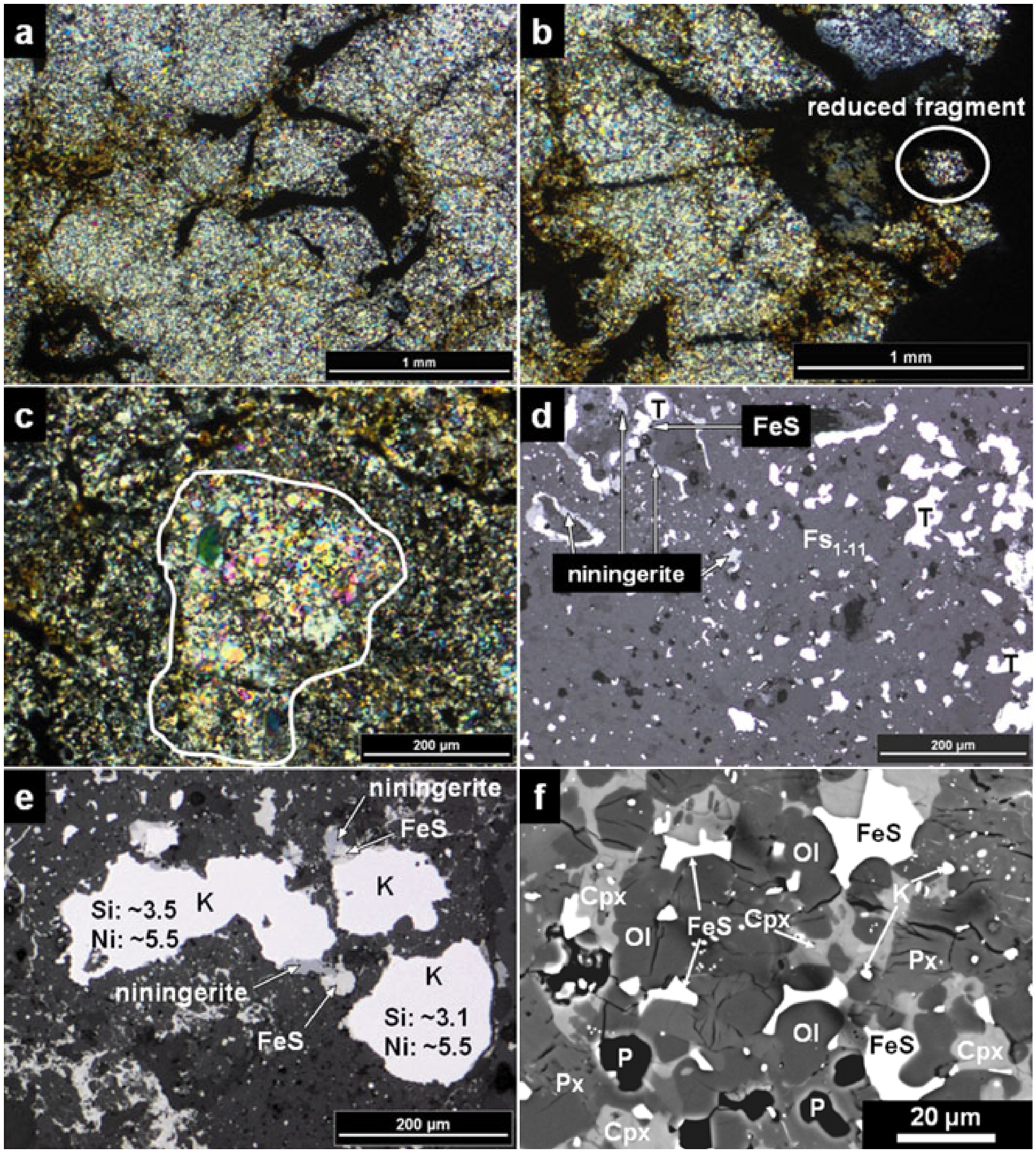

Fig. 1. Fine-grained ureilitic lithologies in Almahata Sitta. a) MS-161: typical fine-grained ureilitic lithology (polarized light, crossed polarizers). b) MS-152: fine-grained lithology with a reduced clast (polarized light, crossed polarizers). c) MS-124: this fine-grained fragment has a coarser-grained ureilitic fragment (polarized light, crossed polarizers). d) MS-165: reflected light photomicrograph of a niningerite-bearing, metal-rich area within the fine-grained ureilitic fragment. FeS = Cr-bearing troilite; K = kamacite. e) MS-20: metal- and sulfide-rich area of the fine-grained ureilitic fragment having niningerite, troilite, and remarkable concentrations of Si and Ni in kamacite (K); reflected light. f) MS-168: low-Ca pyroxene (Px) often occurs intergrown with olivine (Ol), Ca-pyroxene (Cpx), and troilite (FeS) within the fine-grained ureilitic lithology. Ca-pyroxene is mostly an interstitial phase. The tiny white particles are mainly FeS, only some are kamacite (K). P = pores; backscattered electron image.

Walker and Grove 1993; Singletary and Grove 2003; Goodrich et al. 2007; Wilson et al. 2008). Others argue against the smelting model and imply heterogeneous precursor materials instead (e.g., Warren and Huber 2006; Warren 2010). In addition, although most workers now accept that ureilites are partial melt residues (e.g., Boynton et al. 1976; Wasson et al. 1976; Warren and Kallemeyn 1992; Scott et al. 1993; Goodrich 1999), several earlier models explained them as cumulates (Berkley et al. 1980; Goodrich et al. 1987). Takeda (1987) even proposed that ureilites are nebular condensates that underwent high temperature recrystallization during the early stages of planetesimal collision.

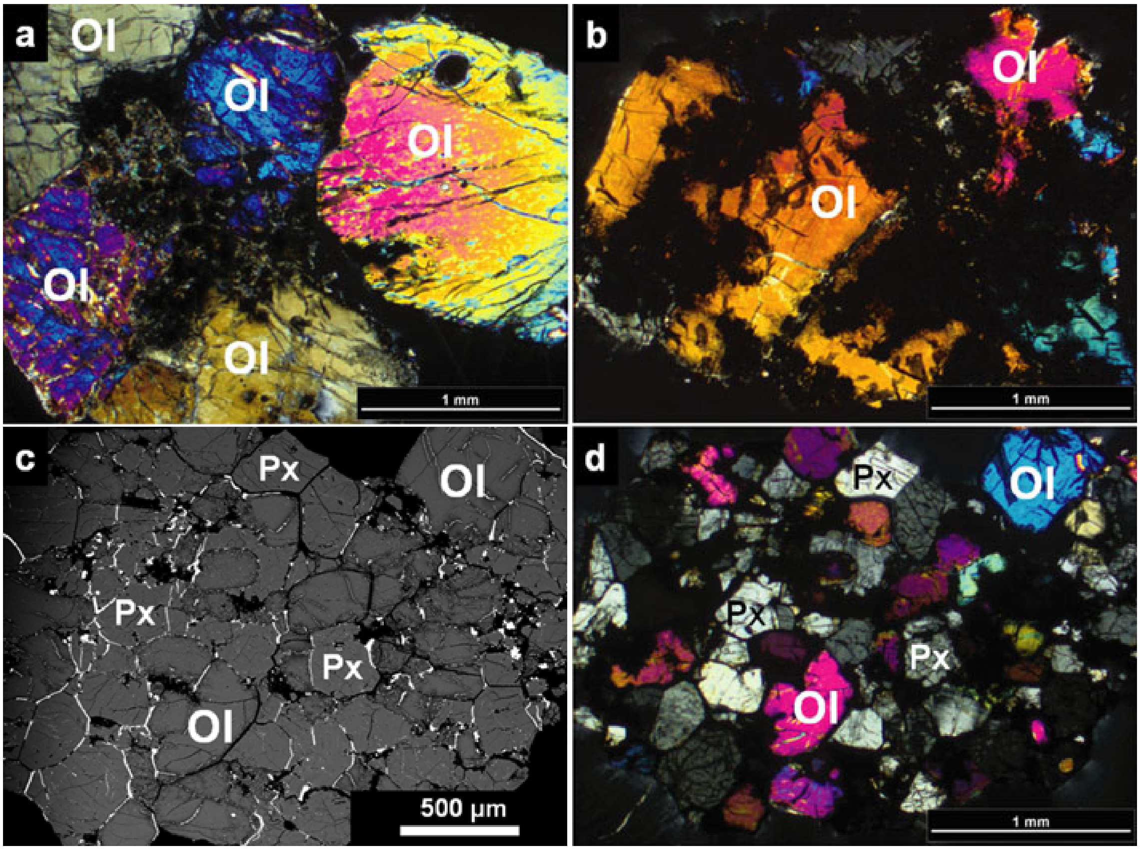

Fig. 2. Different varieties of coarse-grained ureilitic lithologies. a) MS-160 and b) MS-167: typical ureilitic lithology with abundant olivine. c, d) MS-175 (similar area in both images; same minerals are indicated in both images): this type of coarse-grained fragment can be characterized by having abundant pyroxene—most of the gray to dark-gray grains in (c). Grain boundaries are visible based on the distribution of metals and sulfides (white). Photomicrographs were taken in polarized light, crossed polarizers, except the backscattered electron image (c).

The reduction rims surrounding primary mineral grains in ureilites are less controversial. It is believed that they formed by a secondary, late-stage reduction event, probably associated with the disruption of the parent body (e.g., Warren and Kallemeyn 1992; Goodrich et al. 2004).

Oxygen isotope compositions of ureilites fall along a line of slope approximately 1 in a $\delta^{17}O$–$\delta^{18}O$ diagram. This line overlaps with the carbonaceous chondrite anhydrous mineral line (CCAM) defined by Allende calcium-aluminum-rich inclusions and C2–C3 materials (Clayton and Mayeda 1988, 1996). This unique pattern among achondrites reflects oxygen isotope heterogeneity of the ureilite precursor materials.

Among the studied rocks from the Almahata Sitta strewn field, nine samples are ultra-fine-grained ureilites and 11 or 12 are coarse-grained ureilites. One of the coarse-grained specimens may not be a real ureilitic lithology as described below. Two fragments are dominated by metal–sulfide intergrowth having ureilitic lithologies attached or enclosed. All fragments have a similar degree of weathering (Table 1): W0/1 as a maximum (Wlotzka 1993), which is certainly the effect of desert weathering.

The fragments of the fine-grained variety are mineralogically similar to those described by Herrin et al. (2009), Jenniskens et al. (2009), and Zolensky et al. (2009). Typical individual recrystallized olivine grains within these fragments are always below 30 µm, in many cases below 20 µm (Figs. 1a–c and 1f; Table 1). The fine-grained texture of fragment MS-168 is shown in Fig. 1f. Low-Ca pyroxene often occurs intergrown with olivine, Ca-pyroxene, and troilite. Ca-pyroxene is mostly an interstitial phase, and FeS and kamacite occur as grains of variable grain size. Although the bulk fragments are similar in texture to one other, they vary in mineral composition from fragment to fragment (Table 1). Some have olivine core composition of approximately Fa_{12-16} (e.g., MS-28, MS-61, MS-154), whereas others can have olivine core compositions between $\sim Fa_8$ (e.g., MS-20, MS-168) and $\sim Fa_{18-21}$ (e.g., MS-124, MS-152, MS-161; Fig. 1a). One fragment

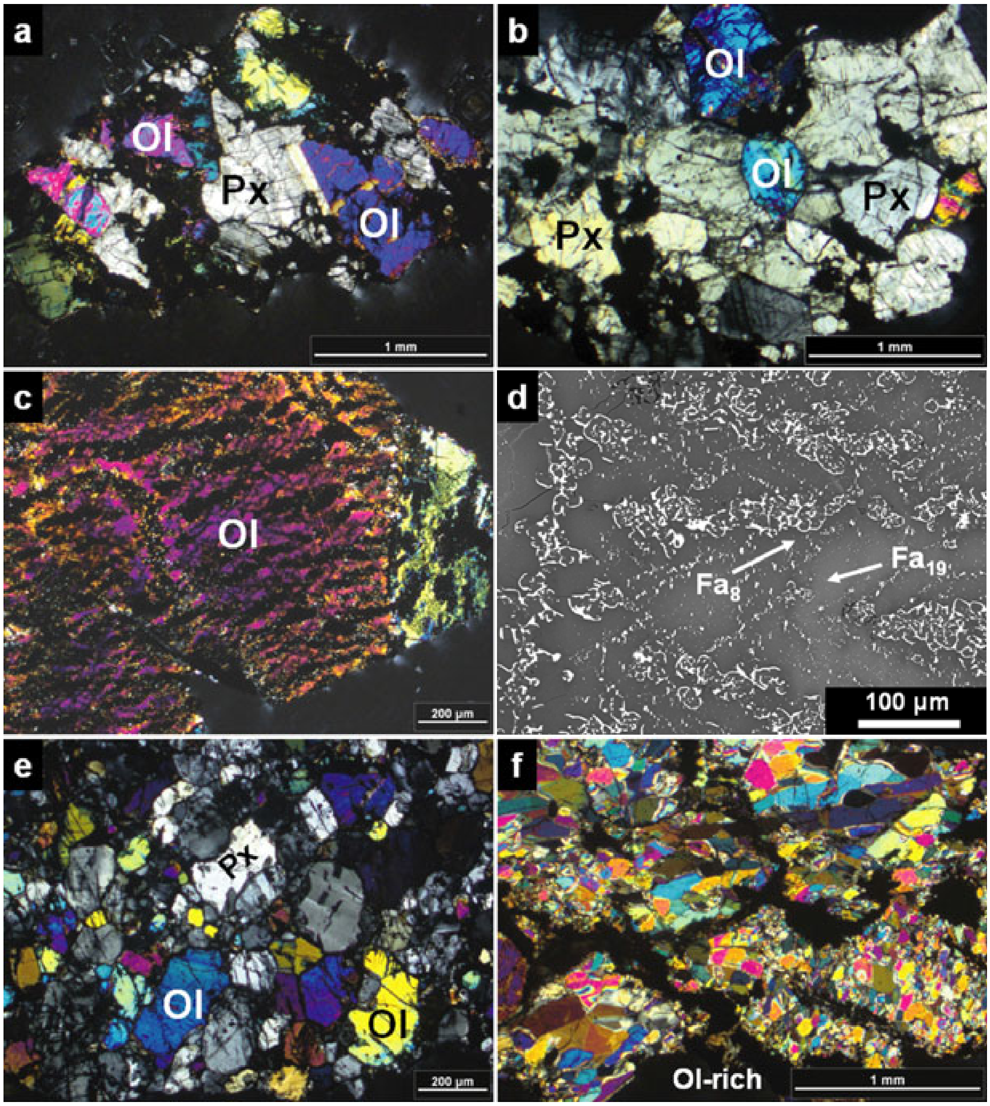

Fig. 3. a) MS-169 is a coarse-grained fragment having abundant pyroxene. b) MS-16: pyroxene-dominating rock. c) MS-156: a unique type of ureilitic lithology with an internal texture (d) showing zoned olivine ($\sim Fa_{8-19}$) and a sulfide/metal network. e) MS-153 and f) MS-171: these fragments have a smaller grain size than the other coarse-grained ureilitic lithologies. Ol = olivine; Fa = fayalite; Px = pyroxene. All photomicrographs were taken in polarized light, crossed polarizers, except for the backscattered electron image of (d).

(MS-152), mainly having olivine of Fa_{18-21}, includes a highly reduced clast with approximately Fa_1 olivines (Fig. 1b). In another case, a fine-grained ureilitic fragment contains a fragment with a significantly larger grain size compared to the surroundings (MS-124; Fig. 1c). The cores of the olivine within the coarser-grained fragment ($\sim Fa_{18-20}$) have a similar composition to those of the fine-grained lithology ($\sim Fa_{19-21}$).

Fragment MS-165 is a niningerite-bearing ureilite (Fig. 1d). Within this fragment, which is dominated by fine-grained ureilitic lithologies, an area was identified, which contains abundant niningerite and metals that have compositions (Ni: ~3.5 wt%, Si: ~4.4 wt%, Co: ~0.3 wt%) similar to those in EH chondrites. As additional phases low-Ca pyroxene (up to En_{99}), Cr-bearing troilite, and a SiO_2-phase were found. Grains of SiO_2 in ureilites were previously reported to occur within the reduced olivine rims (e.g., Weber et al. 2003). Some of the fine-grained ureilitic fragments contain melted areas as indicated by the occurrence of metal and metal/sulfide spherules and the presence of minerals like keilite that occur in enstatite chondrite impact melt rocks and breccias (Keil 2007). A typical specimen is fragment MS-20 containing metal-rich areas having opaques similar to those found in enstatite chondrites: niningerite, keilite, troilite, and

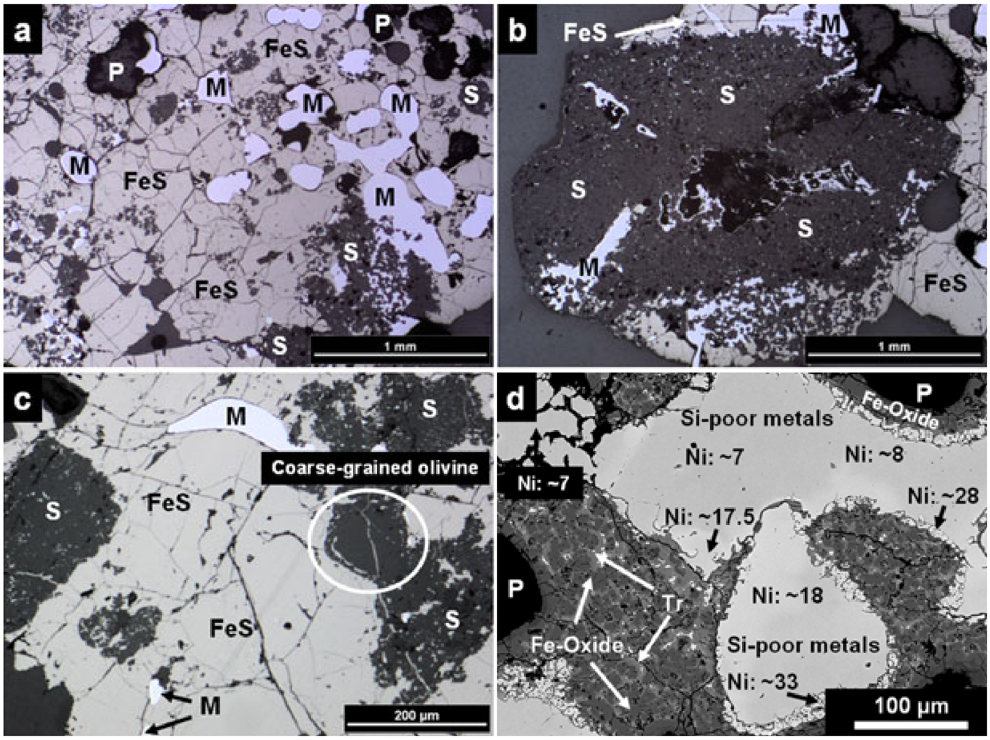

Fig. 4. Fragments dominated by metal–sulfide assemblages. a) The sulfide-metal portion of fragment MS-158 includes highly reduced olivines in the silicate-rich areas (gray). Holes are black (P). b) Fine-grained ureilitic portion attached to the metal–sulfide assemblage of MS-158. c, d) The metal–sulfide assemblage MS-166 is a very porous and mineralogically heterogeneous fragment. The sulfide-rich portion (c) contains inclusions of metal (M), fine-grained ureilitic silicates (S), and a coarse-grained olivine grain; the metal-rich area (d) is surrounded by Ni-rich metals and embedded within an intergrowth of Fe-oxide, sulfide (probably troilite; Tr), and minor metal (white); backscattered electron image. P = pores; M = metals; S = silicates.

metals with about 3.5 wt% Si and about 5.5 wt% Ni (Fig. 1e).

Based on texture and mineral compositions, the coarse-grained ureilites belong to at least six different lithologies of the parent body (Fig. 2). They all have typical grain sizes in excess of 100–300 µm. Some are very coarse grained with olivine grains up to several mm in size (Table 1). Table 1 also contains the compositions of olivine and pyroxene of the samples as well as the degrees of shock and weathering. Based on the shock classification schemes for ordinary and enstatite chondrites (Stöffler et al. 1991; Rubin et al. 1997), all coarse-grained ureilitic fragments are very weakly (S2) or weakly (S3) shocked as indicated by either undulatory extinction or the presence of planar fractures in olivine (Table 1).

Some fragments represent typical ureilites: e.g., MS-160 (Fig. 2a), MS-162, MS-157, MS-167 (Fig. 2b), MS-170. The millimeter-sized olivines within these ureilites have cores of approximately $Fa_{12–22}$ and reduced rims (down to $\sim Fa_1$; Table 1). The four fragments MS-16, MS-169 (Fig. 3a), MS-173, and MS-175 (Figs. 2c and 2d) have abundant pyroxene and the olivines in these fragments have cores with lower fayalite contents ($\sim Fa_5$–$\sim Fa_{11–14}$) than those within the typical coarse-grained, pyroxene-poor variety (Table 1). In fragment MS-16, pyroxene is by far the dominant phase (>80 vol%; Fig. 3b). Based on the mineralogy, it is not certain whether this rock represents an ureilitic lithology or not. The low-Ca pyroxenes are quite uniform in composition ($\sim Fs_{5–6}Wo_{3–4.5}$), whereas the olivines have cores with approximately $Fa_{5–6}$, but show some zoning (Table 1). The metals within the samples have about 4–5 wt% Ni. However, based on oxygen isotope composition MS-16 falls within the ureilite field (see below).

Fragment MS-156 represents a unique type of ureilitic lithology. The huge (>1 mm) olivine grains (Fig. 3c) have a remarkable internal texture with zoned olivines and a fine-grained network of FeS and metals with variable Ni-concentrations (Fig. 3d). The cores of the olivines are approximately Fa_{19}, whereas the olivine close to the sulfide/metal assemblage is $Fa_{<10}$ (Fig. 3d). The Almahata Sitta fragments MS-153 (Fig. 3e) and MS-171 (Fig. 3f) are distinctly smaller grained (typical grain size: 100–300 µm; Table 1) than the rest of the coarse-grained ureilitic lithologies. Both fragments have specific, unique textures: MS-153 contains beside olivine ($\sim Fa_{10–12}$) abundant pyroxene, whereas the olivine grains ($\sim Fa_{15–17}$) in MS-171 show a lineation (Fig. 3f).

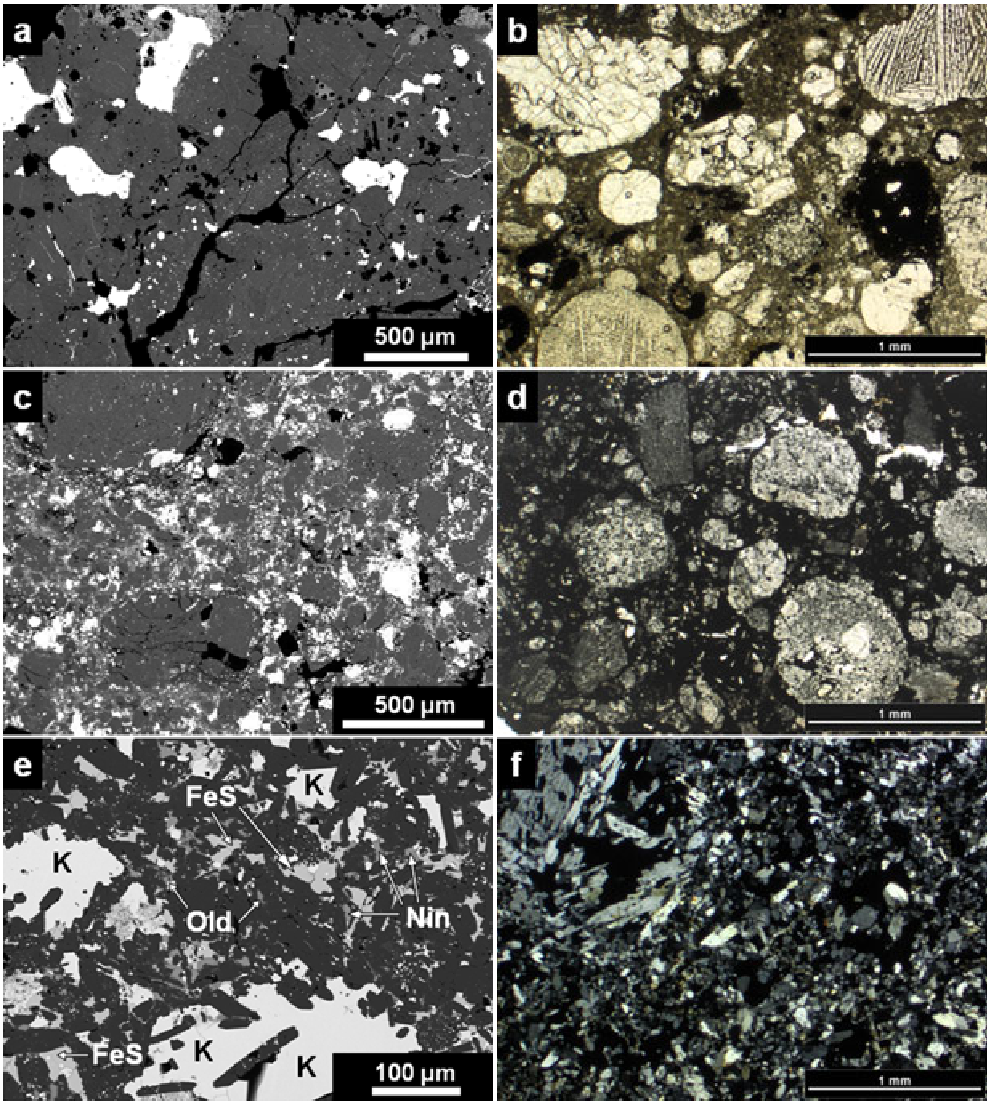

Fig. 5. Chondritic lithologies within the Almahata Sitta polymict breccia. a) MS-11: distribution of metal/sulfides (white) and silicates (gray) within the H5/6 chondrite fragment; the light gray areas in the upper part are parts of the fusion crust. Pores are black; backscattered electron (BSE) image. b) Photomicrograph in transmitted light of the ''unique'' chondrite (MS-CH). c) Overview of the Almahata Sitta fragment MS-14, which is an unequilibrated EH3 chondrite. d) Photomicrograph in transmitted light of the EL3/4 chondrite MS-17. e) The shock-darkened fragment MS-13 is an EH impact melt rock as indicated by the crystal laths. K = kamacite; Old = oldhamite; Nin = niningerite; FeS = troilite; BSE image. f) Typical area of the EL6 chondrite MS-52; transmitted light, crossed polarizers.

Two meteorite fragments are dominated by metals and sulfides. In one case, such a sulfide-metal assemblage (MS-158; Fig. 4a) has an area of fine-grained ureilitic lithology attached (Fig. 4b). Highly reduced olivine is found in silicate inclusions within the sulfide-metal intergrowth. In a second fragment, the sulfide-metal assemblage is very heterogeneous and porous (MS-166). One part is sulfide-rich (troilite) enclosing coarse-grained and fine-grained ureilitic olivine (Fig. 4c). The metal has about 17 wt% Ni. In another area of the fragment, Si-poor metal with variable Ni-concentrations (about 7–20 wt%) dominates (Fig. 4d). These metals are surrounded by small Ni-rich metal grains (~30 wt% Ni) and enclosed in a complex intergrowth of small metals, Ni-bearing sulfides (probably troilites), and Fe-oxides (Fig. 4d).

Mineralogy—Chondritic Lithologies

Of the 17 chondritic fragments identified, 14 belong to different enstatite chondrite groups and two to the ordinary chondrite group (Table 2). Among these

Table 3. Data summary for the detected cosmogenic radionuclides in two samples of the Almahata Sitta meteorite. The reported uncertainties in the last digits (in parentheses) are expanded uncertainties with $k = 1$, the upper limits are given with 90% CL. For data on MS-CH, see also Horstmann et al. (2010).

		Activity concentrations in [dpm kg^{-1}]	
Radionuclide	Half-life	MS-CH (5.1 g)	MS-D (8.65 g)
^{26}Al	717000 yr	57 (12)	75 (8)
^{60}Co	5.2710 yr	22 (5)	84 (6)
^{54}Mn	312.13 days	114 (19)	134 (14)
^{22}Na	2.6027 yr	78 (15)	104 (12)
^{46}Sc	83.788 days	19 (8)	< 22
^{57}Co	271.8 days	22 (10)	16 (3)

Table 4. Results for the naturally occurring nuclides Th, U, and K_{nat} in two samples of the Almahata Sitta meteorite. The reported uncertainties in the last digits (in parentheses) are expanded uncertainties with $k = 1$, the upper limits are given with 90% CL.

	Concentrations in [ng g^{-1}]	
Nuclide	MS-CH (5.1 g)	MS-D (8.65 g)
Th	< 40	20 (7)
U	38 (14)	5 (2)
K_{nat}	$635\ (100) \times 10^3$	$632\ (66) \times 10^3$

chondritic varieties is also a "unique" chondrite—different from typical ordinary, carbonaceous, and Rumuruti (R) chondrites—which will be described in detail by Horstmann et al. (2010). All fragments have a similar degree of weathering (Table 2). Due to differences in texture, mineralogy, and mineral compositions, the 14 enstatite chondrite fragments represent at least six or seven different enstatite chondrites (Table 2): EH3 (MS-14), EL3/4 (MS-17, MS-164), EL6 (MS-52, MS-79), EL breccias (MS-7, MS-D, MS-174), EL impact melt rocks or impact melt breccias (MS-150, MS-159, MS-172), and EH impact melt rocks and breccias (MS-13, MS-155, MS-163). Some of the EH impact melt rocks and breccias are shock-darkened to various degree and may indicate two distinct lithologies. The degree of shock metamorphism of all chondritic samples was determined based on the classification schemes of Stöffler et al. (1991) and Rubin et al. (1997). All samples are very weakly (S2) or weakly (S3) shocked (Table 2).

The two fragments of the H-group ordinary chondrites are different from one another in mineralogy and texture: The H5 (MS-151) and H5/6 (MS-11; Fig. 5a) chondrites have different compositions of olivine and pyroxene ($\sim Fs_{17.5}/\sim Fa_{20.5}$ and $\sim Fs_{14}/\sim Fa_{16.5}$, respectively). The fragment MS-151 is shock-darkened and the texture is barely visible in transmitted light. A higher petrologic type than H5 cannot be ruled out for this fragment. MS-11 contains shock-melted areas as indicated by the occurrence of metal and metal/troilite spherules and opaque assemblages of fine-grained metal–troilite intergrowth.

The "unique" chondrite fragment (MS-CH) is a type 3.8 ± 0.1 chondrite with a chondrule/matrix ratio of about 1.5 (Fig. 5b). Olivine is mainly Fa_{35-37}. As the rock has a considerable abundance of mainly Ni-rich metal (Ni: ~40 wt%, Co: ~2 wt%), a relationship to CK chondrites (e.g., Kallemeyn et al. 1991; Geiger et al. 1993; Geiger and Bischoff 1995) can be ruled out. Based on the mineral chemistry of the silicates, the MS-CH sample has more similarities to R chondrites than to any other chondrite group (e.g., Bischoff et al. 1994; Schulze et al. 1994), but the significant abundance of metal, the lack of NiO in olivine, the lack of PGE-rich phases, and the low TiO_2 concentration of the Cr-spinels demonstrate distinct differences with R chondrites. For details, see Horstmann et al. (2010).

In the following, some of the enstatite chondrite fragments will be characterized in more detail. The basic characteristics of the other fragments can be taken from Table 2. The Si-concentrations of metals in the EH and EL chondrites are distinctly different (Brearley and Jones 1998). Within the EL group, the Si content of kamacite increases from roughly 0.4 wt% in EL3s to 0.9–1.8 wt% in EL5s and finally 1.1–1.7 wt% in EL6s. Within the EH group the Si content of kamacite is about 2 wt% in EH3s, increasing to 2.6–3.5 wt% in EH4s, and roughly 4 wt% in EH6 chondrites (e.g., Keil 1968; Sears et al. 1982; Brearley and Jones 1998; and references therein). These criteria in combination with sulfide mineralogy and textural aspects were used to subdivide the Almahata Sitta E chondrite fragments.

Almahata Sitta fragment MS-14 is a very unequilibrated EH3 chondrite (Fig. 5c), has highly variable compositions of low-Ca pyroxene ($Fs_{0.2-13}$; mean $Fs_{3\pm4}$), and contains minor forsteritic olivine. Preliminary data show that the abundant metals have mean Si-, Co-, and Ni-concentrations of approximately 3.1, 0.7, and 4.2 wt%, respectively. The Ni-concentrations vary from ~3 to ~7 wt%. Other phases include plagioclase, a SiO_2-phase, perryite, schreibersite, troilite, daubreelite, niningerite, and oldhamite.

Fragment MS-17 is an EL3/4 chondrite (Fig. 5d) having abundant chondrules. In some of these chondrules, minor forsteritic olivine occurs. The enstatites contain low, but variable Fe-concentrations (Fs_{0-1}). Preliminary analyses show that the metals have Si-, Co-, and Ni-concentrations of about 0.5, 0.7, and 6.3 wt%, respectively. Other phases include Ca-pyroxene, plagioclase, a SiO_2-phase, graphite, troilite, oldhamite, and alabandite.

Some E chondrite fragments are shock-darkened. Fragment MS-13 is an EH chondrite (Fig. 5e), in which most enstatites have small, but significant Fs-contents (up to 1.6 mole%). Based on the texture, it is probably an impact melt rock (Fig. 5e). The metals have Si-, Co-, and Ni-concentrations of roughly 2.7, 0.7, and 5.5 wt%, respectively. Other phases include plagioclase, a SiO_2-rich phase, troilite, niningerite, oldhamite, and graphite.

Two samples are strongly metamorphosed EL6 chondrites (Fig. 5f). Three fragments are classified as EL chondrite breccias (see fig. 1 in Horstmann and Bischoff 2010a). The presence of keilite indicates that at least some fragments of the breccias are of impact melt origin (Keil 2007; cf. Table 2). The breccia MS-D is a highly recrystallized enstatite-rich rock which contains several clasts up to 5 mm in apparent size. Some of these clasts contain remarkably high abundances of Ca-pyroxene. The metals in MS-D have Si-, Co-, and Ni-concentrations of approximately 0.9, 0.5, and 5.5 wt%, respectively. Other yet identified phases include plagioclase, troilite, oldhamite, Zn-bearing alabandite, and keilite. Based on the texture and the presence of keilite, six impact melt rocks or impact melt breccias (three EH and three EL; Table 2) are among the enstatite chondrite samples. Some mineralogical information on these fragments is given in Table 2.

Table 5. Oxygen isotope composition of Almahata Sitta fragments. Data are reported in ‰ relative to standard mean ocean water.

Fragment no.	Class	Mass (mg)	$\delta^{17}O$	$\delta^{18}O$	$\Delta^{17}O$
MS-16	Ureilite (coarse-grained)	1.60	2.28	6.28	−1.05
MS-169	Ureilite (coarse-grained)	2.08	1.55	6.16	−1.69
MS-170	Ureilite (coarse-grained)	0.85	3.40	7.97	−0.82
MS-175	Ureilite (coarse-grained)	1.22	2.97	7.30	−0.89
MS-20	Ureilite (fine-grained)	1.19	3.99	7.99	−0.23
MS-61	Ureilite (fine-grained)	2.20	3.57	7.94	−0.60
MS-124	Ureilite (fine-grained)	1.22	3.42	7.59	−0.59
MS-168	Ureilite (fine-grained)	2.09	3.80	8.10	−0.48
MS-D	EL6 breccia	3.24	3.06	5.85	−0.01
MS-52	EL6	2.09	3.31	6.27	0.02
MS-79	EL6	1.12	3.31	6.17	0.07
MS-151	H5	1.56	2.93	4.10	0.78
MS-151	H5	1.55	3.03	4.42	0.71
MS-11	H5/6	1.50	3.08	4.35	0.80
MS-CH[a]	"Unique," R-like	3.78	4.35	4.94	1.76

[a]Mean, see Horstmann et al. (2010) for details.

Oxygen Isotope Composition

The oxygen isotope compositions of 14 fragments (six chondritic and eight ureilitic) were determined (Table 5). All ureilite samples (MS-16, -20, -61, -124, -168, -169, -170, and -175) fall on the CCAM line (Fig. 6). Three enstatite chondrite fragments (MS-52, MS-79, and MS-D) fall within uncertainty on the TFL in the enstatite chondrite field. Samples MS-11 and MS-151 were classified as H chondrites. Considering the error limits of the oxygen isotope compositions ($\delta^{18}O = \pm 0.2‰$) these samples are H chondrites, but a slight tendency toward L chondrites is obvious (Fig. 6). The oxygen isotope composition of fragment MS-CH plots at the low $\delta^{17}O$ border of the R-chondrite field and will be discussed in Horstmann et al. (2010).

Cosmogenic Radioisotopes

The measured activity concentrations for the detected cosmogenic radionuclides (^{22}Na, ^{54}Mn, ^{46}Sc, ^{26}Al, ^{57}Co, and ^{60}Co) are given in Table 3. The detection of ^{46}Sc (half-life: 83.8 days) in MS-CH, and of ^{54}Mn (half-life: 312.2 days) and ^{57}Co (half-life: 271.8 days) in both samples clearly indicates that these fragments result from a very recent meteorite fall consistent with the Almahata Sitta event. In particular, the value for ^{46}Sc in MS-CH clearly indicates that this fragment results from a very recent meteorite fall, about 335–420 days prior to the measurement. For the sample MS-D, one can give only a much weaker estimate of the date of fall, using the ^{57}Co and the ^{54}Mn data. The range is 300–600 days based on the available data in the literature for the measured activity concentrations for both radionuclides in chondrites (e.g., Evans et al. 1982). All cosmogenic radioisotopes except ^{60}Co agree within one sigma in the two analyzed fragments. This particular difference can therefore hardly be explained by different shielding positions of the fragments within the same parent body, as more than one radioisotope should be affected. A more plausible explanation seems to be a local inhomogeneous distribution of Co and Ni itself, the most important target materials for the production of this isotope. It could vary up to a factor of 2 with respect to the average values reported for both types in literature. Either there is more Ni and Co in MS-D than in MS-CH or less Ni and Co in MS-CH

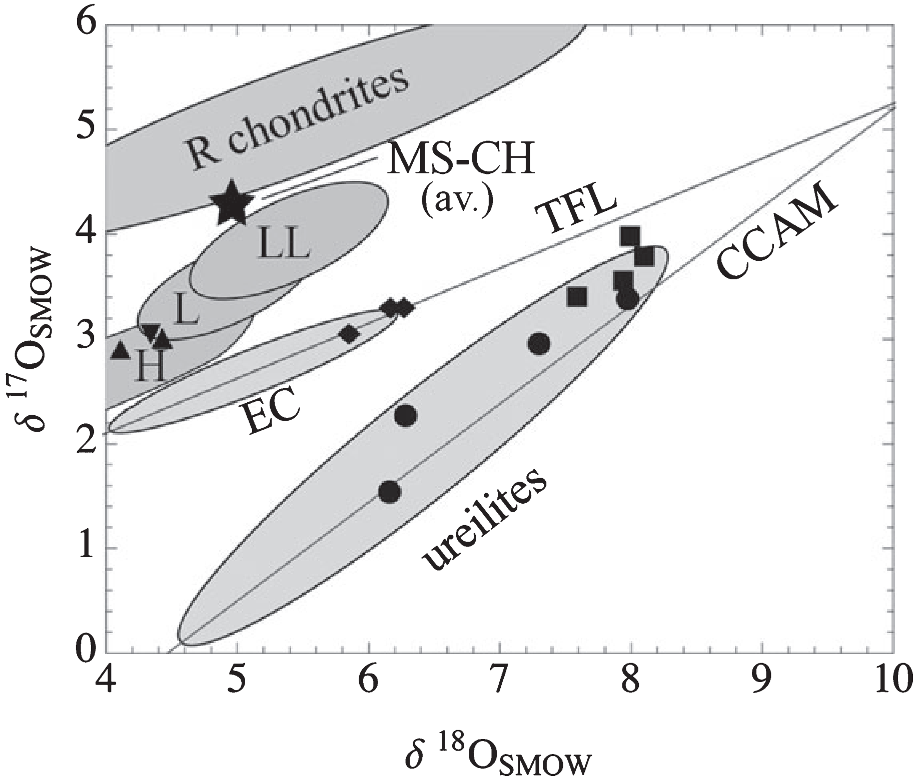

Fig. 6. Plot of $\delta^{17}O$ versus $\delta^{18}O$ of Almahata Sitta fragments (solid squares: fine-grained ureilites, solid circles: coarse-grained ureilites, diamonds: enstatite chondrites, triangles: H chondrites). The fields of O, E, and R chondrites and ureilites are shown for reference. The average of three fragments of MS-CH (“unique”; R-like) is displayed for reference (data from Horstmann et al. 2010). TFL = terrestrial fractionation line; CCAM = carbonaceous chondrite anhydrous mineral line.

with respect to MS-D. The sample masses are rather small and such inhomogeneous distributions start to be important even for gamma spectrometric measurements. Usually, sample masses from 50 g upward are measured, and hence this effect is averaged out over the whole sample. For the different values in ^{60}Co, further analysis is needed to interpret the data correctly. The long-lived spallation product ^{26}Al has reached its saturation activity. The average production rate is well in agreement with the values cited in literature (Bhandari et al. 1993).

The activities measured for the isotopes ^{22}Na, ^{46}Sc, ^{57}Co, and ^{54}Mn are in agreement with what is reported in literature for chondrites (Shedlovsky et al. 1967; Cressy 1972; Mason 1979; Evans et al. 1982).

The concentrations of the natural radionuclides ^{232}Th and ^{238}U as well as for K_{nat} in the meteorite specimens are listed in Table 4. They are well in accordance with the values reported in literature (Wasson and Kallemeyn 1988). Inhomogeneous distribution could also explain why the value for uranium differs by more than one sigma, a significant difference, between the two measured samples.

DISCUSSION

A Common Asteroidal Origin of Chondritic and Ureilitic Lithologies in Almahata Sitta

Although we have short-lived cosmogenic radioisotope data on only two samples, and we do not have oxygen isotope data on all samples, we believe that most, if not all different lithologies described within this study belong to the Almahata Sitta meteorite fall. In the following, we will discuss the “pros” and “cons” of this hypothesis in detail. The main “pro” arguments can be summarized as follows:

1. The detection of the short- and medium short-lived cosmogenic nuclides ^{46}Sc, ^{57}Co, and ^{54}Mn clearly indicates that the chondritic fragments MS-CH and MS-D result from a fresh meteorite fall consistent with the Almahata Sitta event in October 2008. In this respect, it is important to mention that these two samples are mineralogically completely different from each other and also different from the main ureilitic lithologies from the Almahata Sitta strewn field.

2. No sample has a weathering degree higher than W0/1 as indicated by the only slight brownish taint in transmitted light and/or by only very thin rinds of weathering products surrounding the metal grains (Tables 1 and 2). Thus, all samples have a very similar degree of weathering.
3. Although most small fragments from the strewn field appear to represent fragments of a single lithology, preliminary studies show that at least some fragments contain two different lithologies (e.g., MS-124, MS-152, MS-158, MS-166; see above).
4. Among the fragments at least seven different E chondrite lithologies were detected. Considering the actual meteorite flux, about 75% of meteorite falls (more than 90% of the chondrite falls) represent ordinary chondrites. Enstatite chondrites are relatively rare (below 2% of the actual meteorite flux) and such a high number of fresh, different E chondrite meteorite falls in just one small area can only be explained with a common origin in the asteroid 2008 TC_3. Even if we consider EL and EH chondrite breccias in both cases, we would need at least two different E chondrite fall events.
5. Meteorite falls are usually eyewitnessed by many local people. For the many different rock types found within the Almahata Sitta strewn field, a considerable number of recent meteorite falls (at least six!) is required. However, such eyewitness reports do not exist.
6. The discovery of several new unique meteorite fragments (having so far unknown textures and mineralogy; e.g., MS-CH, MS-166, and MS-158) in a small area is best explained with a breakup of a polymict asteroid.

Nevertheless, it remains to demonstrate definitively that all fragments from the Almahata Sitta strewn field were components of asteroid 2008 TC_3. Because of the lack of short-lived cosmogenic radioisotope data on all studied fragments there is still some uncertainty. As more than 90% of chondrite falls are ordinary chondrites, considering fall statistics at least for the ordinary chondrite group a certain chance of a recent fall exists. We mentioned above that meteorite falls are usually seen by many eyewitnesses. This may not be the case in the relatively uninhabitated desert area of Sudan.

Considering all "pros" and "cons," and available data, we suggest that it is most likely that all the different chondritic and achondritic components so far found in the Almahata Sitta strewn field have a common origin in asteroid 2008 TC_3.

The ureilite fragments fall in the ureilite field in a 3-oxygen isotope diagram (Fig. 6). They do not, however, show any systematic relationship between $\Delta^{17}O$ and Fa-content of the olivine (cf. Tables 1 and 5), as has been described for other ureilites (e.g., Mittlefehldt et al. 1998). The fine-grained ureilites cluster at high $\Delta^{17}O$, whereas the coarse-grained ureilite fragments are more ^{16}O-rich (Fig. 6). The E chondrite fragments all fall within error on the TFL in the E chondrite field (Fig. 6) supporting the petrological classification. The H chondrites fall within the ordinary chondrite field. The oxygen isotopes of fragment MS-CH (see Horstmann et al. 2010) are closely linked to R chondrites. The result illustrates that the Almahata Sitta breccia is fragmented on a very small scale.

Mixing of Different Rock Types in Asteroids—Fragments in Chondrites

Studies of shock effects in meteorites and breccias are extremely important for providing information on the evolution of asteroidal parent bodies (e.g., Bischoff et al. 1983, 2006; Bunch and Rajan 1988; Stöffler et al. 1988, 1991; Lipschutz et al. 1989; Bischoff and Stöffler 1992; Rubin 1997; Rubin et al. 1997). The existence and abundance of foreign and exotic fragments in meteorites give some measure of the degree of mixing among asteroids in the asteroidal belt. In addition, the relative abundance of different types of material in different meteorite breccias may reveal something about the abundance of certain materials at different times and places in the asteroid belt. One of the most complex meteorite breccias is Kaidun (Zolensky and Ivanov 2003), which will be described below; however, only a few meteorites contain more than a few volume percent of foreign clasts and the most abundant clasts are CM-like chondritic fragments (Fodor et al. 1976; Meibom and Clark 1999; Bischoff et al. 2006).

In ordinary chondrite breccias, fragments from other ordinary chondrite groups are very rare and are summarized in Bischoff et al. (2006). These include: (1) intensely shocked H-group chondrite fragments in the LL chondrite St. Mesmin (Dodd 1974); (2) an LL5 clast in the Dimmitt H chondrite regolith breccia (Rubin et al. 1983); (3) an L-group melt rock fragment in the LL chondrite Paragould (Fodor and Keil 1978); (4) fragments in Adzhi-Bogdo (LL3–6), which appear to derive from L-group chondrites (Bischoff et al. 1993, 1996); (5) a troctolitic clast with an H chondrite oxygen isotopic composition in the Yamato-794046 (L6) chondrite (Prinz et al. 1984); (6) an L chondritic inclusion in the Fayetteville H chondrite regolith breccia (Wieler et al. 1989); and (7) a fragment of H chondrite parentage within the Ngawi LL chondrite (Fodor and Keil 1975).

CM-type fragments occur in different groups of chondrites: A small CM chondrite clast with a matrix of phyllosilicates and sulfides was observed in the

Magombedze (H3–5) chondrite breccia (MacPherson et al. 1993). In addition, carbonaceous clasts were described to occur in the H-group ordinary chondrite breccia Dimmitt (Rubin et al. 1983) and the H-group chondrites Abbott and Plainview (Rubin and Bottke 2009). Other possible carbonaceous clasts in various ordinary chondrites are given by Keil (1982).

In addition, some achondritic clasts have been reported in brecciated chondrites (e.g., Hutchison et al. 1988; Fredriksson et al. 1989; Bischoff et al. 1993, 2006; Bridges and Hutchison 1997; Sokol et al. 2007a, 2007b; Terada and Bischoff 2009).

Mixing of Different Rock Types in Asteroids—Fragments in Achondrites

Carbonaceous chondrite clasts mineralogically similar to CM and CV3 chondrites have been reported in several polymict HED breccias (e.g., Kapoeta and Lewis Cliff 85300) by Wilkening (1973) and Zolensky et al. (1992, 1996). The occurrence of other types of chondritic clasts in brecciated HED achondrites was further reported by Bunch et al. (1979), Kozul and Hewins (1988), Mittlefehldt and Lindstrom (1988), Hewins (1990), Reid et al. (1990), Buchanan et al. (1993), Mittlefehldt (1994), Pun et al. (1998), and Buchanan and Mittlefehldt (2003).

Ordinary chondrite fragments have been found in polymict ureilites (e.g., Jaques and Fitzgerald 1982; Prinz et al. 1986, 1987, 1988; Ikeda et al. 2000, 2003; Goodrich et al. 2004; Ross et al. 2010). Angrite-like clasts have also been reported in several polymict ureilites (e.g., Jaques and Fitzgerald 1982; Prinz et al. 1986, 1987; Ikeda et al. 2000; Goodrich and Keil 2002; Cohen et al. 2004; Kita et al. 2004). Fine-grained dark clasts mineralogically similar to fine-grained carbonaceous chondrite material are also known to exist in some polymict ureilites (e.g., Prinz et al. 1987; Brearley and Prinz 1992; Ikeda et al. 2000, 2003; Goodrich and Keil 2002). Recently, some ureilites have been recognized to have impact-melted areas, indicating severe melting and mixing on the ureilite parent body (Warren and Rubin 2006; Janots et al. 2009, Forthcoming). These previously reported occurrences of mixed chondritic and ureilitic components are important in considering the mineralogical and lithological make-up of asteroid 2008 TC_3 studied here.

Formation of Asteroid 2008 TC_3

Bischoff et al. (2006) concluded that ''asteroids are generally modified by two kinds of hypervelocity impacts: frequent impacts that crater the surface, and large rare impacts that damage the whole asteroid and create large volumes of rubble.'' A major fraction of meteorite breccias is created by these large impacts (e.g., Scott 2002; Scott and Wilson 2005). Meteorites containing foreign clasts are typically regolith breccias, but the absence of solar wind gases excludes the possibility that Almahata Sitta is a regolith breccia (Ott et al. 2010). As shown in this study, Almahata Sitta has at least 10 different ureilitic lithologies and at least another 10 different—in one case ''unique'' (Horstmann et al. 2010)—chondritic rock types. Based on our own and available data, most of the Almahata Sitta fragments appear to be of ureilitic origin supporting the classification of the meteorite as a polymict ureilite. In fact, no other ''normal'' polymict ureilite has such a high abundance of exotic clasts. Considering the 10 ureilitic lithologies and their extraordinary diversity alone, it is clear that the coexistence of these lithologies in Almahata Sitta can only be the result of a gigantic and catastrophic disruption and breakup of the ureilite parent body delivering and producing all these different ureilitic lithologies (Fig. 7). Goodrich et al. (2004) discuss the scenario that the delivered material possibly reaccreted into second-generation asteroids of mixed ureilitic material, and that these offspring bodies are sampled by the current ureilite collection. We suggest that at the time of accretion of second-generation asteroid(s), all sorts of chondritic fragments may have been present in a debris disk around the Sun. The chondritic and ureilitic components were mixed and accreted to a second-generation asteroid parental to asteroid 2008 TC_3. Clearly, 2008 TC_3 is part of a second-generation asteroid. From the study of Almahata Sitta fragments, we have no information about the presence of primordial dust in the region of reaccretion. As most of the studied fragments consist of a single lithology, we suggest that the highly porous, fine-grained ureilite material described in Almahata Sitta by Jenniskens et al. (2009) may represent only the weak and relatively unconsolidated matrix (probably of low modal abundance) which surrounded the monolithic clasts. Our studied small fragments—especially the chondritic ones—are not porous and are presumably not inherently weak. Considering the Almahata Sitta bulk rock in general, we have no information on the strength and lithological connections of the various chondritic and achondritic components in Almahata Sitta. Therefore, Almahata Sitta is very different from other polymict ureilites: In other polymict samples, ureilitic and exotic (chondritic) components can be found well-consolidated in one thin section. In addition, other polymict ureilites do not contain such an apparent abundance of ''exotic'' clasts, as it is the case for Almahata Sitta. Enstatite chondrites and unusual fragments with affinities to R chondrites have never been reported to occur as clasts in polymict ureilites. We suggest that Almahata Sitta was

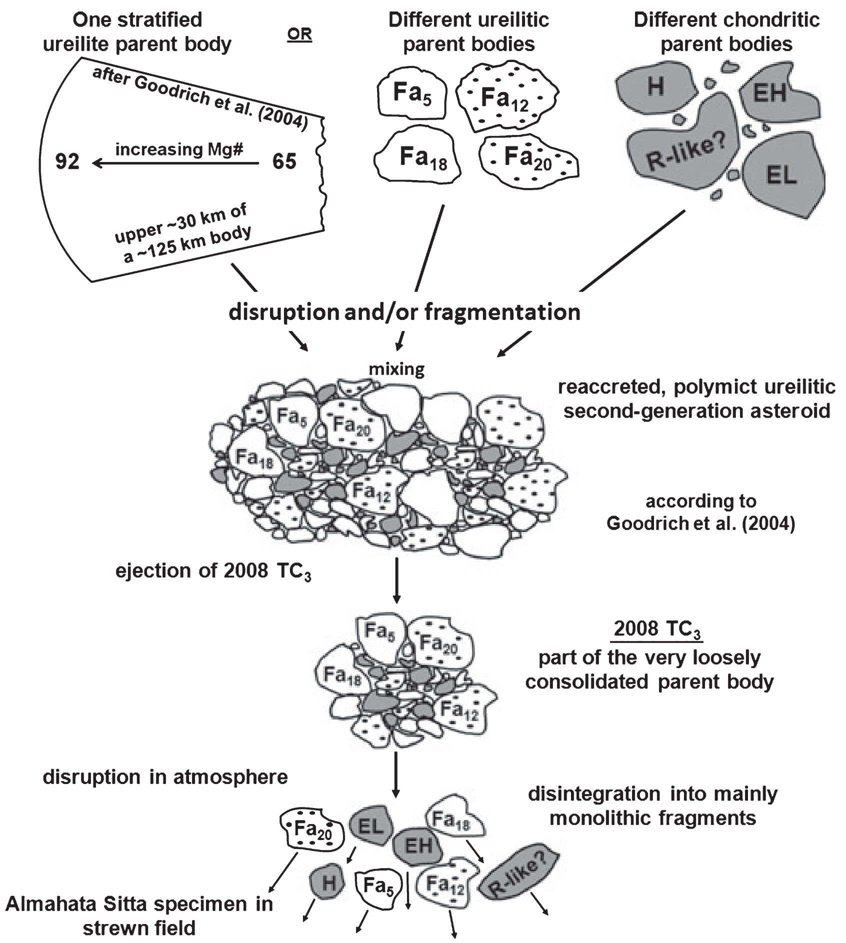

Fig. 7. Possible schematic scenario for the formation and evolution of asteroid 2008 TC_3 and Almahata Sitta. The ‘‘one stratified ureilite parent body’’ assumes the equilibrium smelting model. Considering the formation of asteroid 2008 TC_3 by mixing of various ureilitic and chondritic lithologies we favor a single ureilite parent body starting condition. White, coarse-grained ureilitic lithologies; stippled, fine-grained ureilitic constituents; gray, chondritic components.

much more loosely lithified and porous than Kaidun (Zolensky and Ivanov 2003), which is a well-consolidated breccia, in which the relationship between different lithologies can be studied in much more detail than in the case of Almahata Sitta. Asteroid 2008 TC_3 probably consisted of centimeter-sized(?), loosely agglomerated components that broke up mainly into monolithic fragments along their original boundaries during breakup in the atmosphere (Fig. 7) (Horstmann and Bischoff 2010b).

Kaidun—Probably the Closest Analog to Almahata Sitta

The Kaidun breccia basically consists of chondritic components and not of achondritic constituents. But, based on the huge variety of different types of chondritic fragments, we suggest that Kaidun is the closest known analog to Almahata Sitta. Based on the exceptional variety of rock types, Zolensky and Ivanov (2003) characterized the Kaidun microbreccia as a ‘‘harvest from the inner and outer asteroid belt.’’ Kaidun consists almost entirely of millimeter- and sub-millimeter-sized fragments of EH3–5, EL3, CV3, CM1–2, and R chondrites (Ivanov 1989; Ivanov et al. 2003; Zolensky and Ivanov 2003, and references therein), contains C1 and C2 lithologies, fragments of impact melt products, new enstatite-bearing clasts, phosphide-bearing fragments, clasts of Ca-rich achondrite, possibly aubritic materials, and alkaline-enriched clasts (Ivanov 1989; Ivanov et al. 2003; Zolensky and Ivanov 2003; Kurat et al. 2004). The alkaline-enriched clasts are similar to the granitoidal clasts found in the Adzhi-Bogdo ordinary chondrite regolith breccia (Bischoff et al. 1993, 1996; Sokol and Bischoff 2006; Sokol et al. 2007a, 2007b; Terada and Bischoff 2009). In addition, a possible ordinary chondrite clast has been characterized by Mikouchi et al. (2005). Thus, after the polymict breccia Kaidun (Zolensky and

Ivanov 2003) Almahata Sitta is a new extraordinary breccia for future studies. The coexistence of many different types of clasts in Kaidun supports our hypothesis that most, if not all, studied fragments derive from asteroid 2008 TC_3.

The Mismatch in Reflectance Spectra

According to Gaffey et al. (1993), ureilites should be derived from S-type asteroids. These authors distinguish between pyroxene-poor ureilites (class S(I)), clinopyroxene-bearing ureilites (class S(II)), clinopyroxene and orthopyroxene-bearing ureilites (class S(III)), and orthopyroxene-bearing ureilites (class S(IV)). However, the reflectance spectra of asteroid 2008 TC_3 are similar to those of B- and F-type asteroids (Jenniskens et al. 2009). Based on Gaffey et al. (1993), type B asteroids should contain iron-poor hydrated silicates and type F asteroids should have hydrated silicates and organics. Jenniskens et al. (2009) did not find hydrated silicates in the Almahata Sitta meteorite sample, but came to the somewhat surprising conclusion that Almahata Sitta is similar to a type F asteroid. The asteroid 2008 TC_3 analyzed in space was a mixture of very different lithologies. It is not certain that all its different lithologies have been recognized yet. They probably have not. Perhaps lithologies with hydrated silicates also existed within asteroid 2008 TC_3. Based on the findings presented in this study, the reflectance spectrum of asteroid 2008 TC_3 should be re-evaluated.

Acknowledgments—We thank U. Heitmann (Münster) for sample preparation. N. Albrecht (Göttingen) is thanked for the preparation of the oxygen isotope analyses, and Ed Scott (University of Hawaii) for interesting discussions on the possible accretion scenario of asteroid 2008 TC_3. We also thank the referees Klaus Keil, Alan Rubin, and Harold Connolly for constructive reviews, and the associate editor Cyrena Goodrich for thoughtful comments and discussions.

Editorial Handling—Dr. Cyrena Goodrich

REFERENCES

Berkley J. L. and Jones J. H. 1982. Primary igneous carbon in ureilites: Petrological implications. Proceedings, 13th Lunar and Planetary Science Conference. pp. A353–A364.

Berkley J. L., Taylor G. J., Keil K., Harlow G. E., and Prinz M. 1980. The nature and origin of ureilites. *Geochimica et Cosmochimica Acta* 44:1579–1597.

Bhandari N., Mathew K. J., Rao M. N., Herpers U., Bremer K., Vogt S., Wölfli W., Hofmann H. J., Michel R., Bodemann R., and Lange H.-J. 1993. Depth and size dependence of cosmogenic nuclide production rates in stony meteoroids. *Geochimica et Cosmochimica Acta* 57:2361–2375.

Bischoff A. and Stöffler D. 1992. Shock metamorphism as a fundamental process in the evolution of planetary bodies: Information from meteorites. *European Journal of Mineralogy* 4:707–755.

Bischoff A., Rubin A. E., Keil K., and Stöffler D. 1983. Lithification of gas-rich chondrite regolith breccias by grain boundary and localized shock melting. *Earth and Planetary Science Letters* 66:1–10.

Bischoff A., Geiger T., Palme H., Spettel B., Schultz L., Scherer P., Schlüter J., and Lkhamsuren J. 1993. Mineralogy, chemistry, and noble gas contents of Adzhi-Bogdo—An LL3–6 chondritic breccia with L-chondritic and granitoidal clasts. *Meteoritics* 28:570–578.

Bischoff A., Geiger T., Palme H., Spettel B., Schultz L., Scherer P., Loeken T., Bland P., Clayton R. N., Mayeda T. K., Herpers U., Meltzow B., Michel R., and Dittrich-Hannen B. 1994. Acfer 217—A new member of the Rumuruti chondrite group (R). *Meteoritics* 29:264–274.

Bischoff A., Gerel O., Buchwald V. F., Spettel B., Loeken T., Schultz L., Weber H. W., Schlüter J., Baljinnyam L., Borchuluun D., Byambaa C., and Garamjav D. 1996. Meteorites from Mongolia. *Meteoritics & Planetary Science* 31:152–157.

Bischoff A., Scott E. R. D., Metzler K., and Goodrich C. A. 2006. Nature and origins of meteoritic breccias. In *Meteorites and the early solar system II*, edited by Lauretta D. S. and McSween H. Y. Jr. Tucson, AZ: The University of Arizona Press. pp. 679–712.

Bischoff A., Horstmann M., Laubenstein M., and Haberer S. 2010. Asteroid 2008 TC_3—Almahata Sitta: Not only a ureilitic meteorite, but a breccia containing many different achondritic and chondritic lithologies (abstract #1763). 41st Lunar and Planetary Science Conference. CD-ROM.

Boynton W. V., Starzyk P. M., and Schmitt R. A. 1976. Chemical evidence for genesis of ureilites, achondrite chassigny, and nakhlites. *Geochimica et Cosmochimica Acta* 40:1439–1447.

Brearley A. J. and Jones R. H. 1998. Chondritic meteorites. In *Planetary materials*, edited by Papike J. J. Reviews in mineralogy vol. 26, Washington, D.C.: Mineralogical Society of America. pp. 3-01–3-398.

Brearley A. J. and Prinz M. 1992. CI chondrite-like clasts in the Nilpena polymict ureilite. Implications for aqueous alteration processes in CI chondrites. *Geochimica et Cosmochimica Acta* 56:1373–1386.

Bridges J. C. and Hutchison R. 1997. A survey of clasts and chondrules in ordinary chondrites. *Meteoritics & Planetary Science* 32:389–394.

Buchanan P. C. and Mittlefehldt D. W. 2003. Lithic components in the paired howardites EET 87503 and EET 87513: Characterization of the regolith of 4 Vesta. *Antarctic Meteorite Research* 16:128–151.

Buchanan P. C., Zolensky M. E., and Reid A. M. 1993. Carbonaceous chondrite clasts in the howardites Bholghati and EET 87513. *Meteoritics* 28:659–669.

Bunch T. E., and Rajan R. S. 1988. Meteorite regolith breccias. In *Meteorites and the early solar system*, edited by Kerridge J. F. and Matthews M. S. Tucson, AZ: The University of Arizona Press. pp. 144–164.

Bunch T. E., Chang S., Frick U., Neil J., and Moreland G. 1979. Carbonaceous chondrites—I. Characterization and significance of carbonaceous chondrite (CM) xenoliths in the Jodzie howardite. *Geochimica et Cosmochimica Acta* 43:1727–1742.

Clayton R. N. and Mayeda T. K. 1988. Formation of ureilites by nebular processes. *Geochimica et Cosmochimica Acta* 52:1313–1318.

Clayton R. N. and Mayeda T. K. 1996. Oxygen-isotope studies of achondrites. *Geochimica et Cosmochimica Acta* 60:1919–2018.

Cohen B. A., Goodrich C. A., and Keil K. 2004. Feldspathic clast populations in polymict ureilites: Stalking the missing basalts from the ureilite parent body. *Geochimica et Cosmochimica Acta* 68:4249–4266.

Cressy P. J. Jr. 1972. Cosmogenic radionuclides in the Allende and Murchison carbonaceous chondrites. *Journal of Geophysical Research* 77:4905–4911.

Dodd R. T. 1974. Petrology of the St. Mesmin chondrite. *Contributions to Mineralogy and Petrology* 46:129–145.

Evans J. C., Reeves J. H., Rancitelli L. A., and Bogard D. D. 1982. Cosmogenic nuclides in recently fallen meteorites: Evidence for galactic cosmic ray variations during the period 1967–1978. *Journal of Geophysical Research* 87:5577–5591.

Fodor R. V. and Keil K. 1975. Implications of poikilitic textures in LL-group chondrites. *Meteoritics* 10:325–340.

Fodor R. V. and Keil K. 1978. *Catalog of lithic fragments in LL-group chondrites*. Special Publication No. 19. Albuquerque, New Mexico: Institute of Meteoritics, University of New Mexico. 38 p.

Fodor R. V., Keil K., Wilkening L. L., Bogard D. D., and Gibson E. K. 1976. Origin and history of a meteorite parent-body regolith breccia: Carbonaceous and noncarbonaceous lithic fragments in the Abbott, New Mexico chondrite. In *Tectonics and mineral resources of southwestern New Mexico*, edited by Woodward L. A. and Northrop S. A. Special Publication 6. Socorro, New Mexico: New Mexico Geological Society. pp. 206–218.

Fredriksson K., Jarosewich E., and Wlotzka F. 1989. Study Butte: A chaotic chondrite breccia with normal H-group chemistry. *Zeitschrift für Naturforschung* 44a:945–962.

Gaffey M. J., Burbine T. H., and Binzel R. P. 1993. Asteroid spectroscopy: Progress and perspectives. *Meteoritics* 28:161–187.

Geiger T. and Bischoff A. 1995. Formation of opaque minerals in CK chondrites. *Planetary and Space Science* 43:485–498.

Geiger T., Spettel B., Clayton R. N., Mayeda T. K., and Bischoff A. 1993. Watson 002—the first CK—type 3 chondrite. *Meteoritics* 28:352.

Goodrich C. A. 1999. Are ureilites residues from partial melting of chondritic material? The answer from MAGPOX. *Meteoritics & Planetary Science* 34:109–117.

Goodrich C. A. and Keil K. 2002. Feldspathic and other unusual clasts in polymict ureilite DaG 165 (abstract #1777). 33rd Lunar and Planetary Science Conference. CD-ROM.

Goodrich C. A., Jones J. H., and Berkley J. L. 1987. Origin and evolution of the ureilite parent magma: Multi-stage igneous activity on a large parent body. *Geochimica et Cosmochimica Acta* 51:2255–2273.

Goodrich C. A., Scott E. R. D., and Fioretti A. M. 2004. Ureilitic breccias: Clues to the petrologic structure and impact disruption of the ureilite parent asteroid. *Chemie der Erde—Geochemistry* 64:283–327.

Goodrich C. A., Van Orman J., and Wilson L. 2007. Fractional melting and smelting on the ureilite parent body. *Geochimica et Cosmochimica Acta* 71:2876–2895.

Herrin J. S., Zolensky M. E., Ito M., Jenniskens P., and Shaddad M. H. 2009. Fossilized smelting: Reduction textures in Almahata Sitta ureilite (abstract). *Meteoritics & Planetary Science* 44:A89.

Hewins R. H. 1990. Geologic history of LEW 85300, 85302 and 85303 polymict eucrites (abstract). 21st Lunar and Planetary Science Conference. pp. 509–510.

Horstmann M. and Bischoff A. 2010a. Characterization of spectacular lithologies from the Almahata Sitta breccia (abstract #1784). 41st Lunar and Planetary Science Conference. CD-ROM.

Horstmann M. and Bischoff A. 2010b. Formation and evolution of the highly unconsolidated asteroid 2008 TC_3. *Meteoritics & Planetary Science* 45:A83.

Horstmann M., Bischoff A., Pack A., and Laubenstein M. 2010. Almahata Sitta—fragment MS-CH: Characterization of a new chondrite type. *Meteoritics & Planetary Science* 45. This issue.

Hutchison R., Williams C. T., Din V. K., Clayton R. N., Kirschbaum C., Paul R. L., and Lipschutz M. E. 1988. A planetary, H-group pebble in the Barwell, L6, unshocked chondritic meteorite. *Earth and Planetary Science Letters* 90:105–118.

Ikeda Y., Prinz M., and Nehru C. E. 2000. Lithic and mineral clasts in the Dar al Gani (DaG) 319 polymict ureilite. *Antarctic Meteorite Research* 13:177–221.

Ikeda Y., Kita N. T., Morishita Y., and Weisberg M. K. 2003. Primitive clasts in the Dar al Gani 319 polymict ureilite: Precursors of the ureilites. *Antarctic Meteorite Research* 16:105–127.

Ivanov A. V. 1989. The Kaidun meteorite: Composition and history. *Geochemistry International* 26:84–91.

Ivanov A. V., Kononkova N. N., Yang A. V., and Zolensky M. E. 2003. The Kaidun meteorite: Clasts of alkaline-rich fractionated materials. *Meteoritics & Planetary Science* 38:725–737.

Janots E., Gnos E., Hofmann B. A., Greenwood R. C., Franchi I. A., and Bischoff A. 2009. Jiddat al Harasis 422: The first ureilitic impact melt breccia (abstract). *Meteoritics & Planetary Science* 44:A100.

Janots E., Gnos E., Hofmann B. A., Greenwood R. C., Franchi I. A., and Bischoff A. Forthcoming. Jiddat al Harasis 422: A ureilite with an extremely high degree of shock melting. *Meteoritics & Planetary Science* 46.

Jaques A. L. and Fitzgerald M. J. 1982. The Nilpena ureilite, an unusual polymict breccia—Implications for origin. *Geochimica et Cosmochimica Acta* 46:893–900.

Jenniskens P., Shaddad M. H., Numan D., Elsir S., Kudoda A. M., Zolensky M. E., Le L., Robinson G. A., Friedrich J. M., Rumble D., Steele A., Chesley S. R., Fitzsimmons A., Duddy S., Hsieh H. H., Ramsay G., Brown P. G., Edwards W. N., Tagliaferri E., Boslough M. B., Spalding R. E., Dantowitz R., Kozubal M., Pravec P., Borovička J., Charvat Z., Vaubaillon J., Kuiper J., Albers J., Bishop J. L., Mancinelli R. L., Sandford S. A., Milam S. N., Nuevo M., and Worden S. P. 2009. The impact and recovery of asteroid 2008 TC_3. *Nature* 458:485–488.

Kallemeyn G. W., Rubin A. E., and Wasson J. T. 1991. The compositional classification of chondrites: V. The Karoonda (CK) group of carbonaceous chondrites. *Geochimica et Cosmochimica Acta* 55:881–892.

Keil K. 1968. Mineralogical and chemical relationships among enstatite chondrites. *Journal of Geophysical Research* 73:6945–6976.

Keil K. 1982. Composition and origin of chondritic breccias. In *Workshop on lunar breccias and soils and their meteoritic analogs*, edited by Taylor G. J. and Wilkening L. L. LPI Technical Report 82-02. Houston, Texas: Lunar Planetary Institute. pp. 65–83.

Keil K. 2007. Occurrence and origin of keilite, $(Fe_{>0.5},Mg_{<0.5})S$, in enstatite chondrite impact melt rocks and impact melt breccias. *Chemie der Erde—Geochemistry* 67:37–54.

Kita N. T., Ikeda Y., Togashi S., Liu Y., Morishita Y., and Weisberg M. K. 2004. Origin of ureilites inferred from a SIMS oxygen isotopic and trace element study of clasts in the Dar al Gani 319 polymict ureilite. *Geochimica et Cosmochimica Acta* 68:4213–4235.

Kozul J. and Hewins R. H. 1988. LEW 85300,02,03 polymict eucrites consortium—II: Breccia clasts, CM inclusions, glassy matrix and assembly history (abstract). 19th Lunar and Planetary Science Conference. pp. 647–648.

Kurat G., Zinner E., Brandstätter F., and Ivanov A. V. 2004. Enstatite aggregates with niningerite, heideite, and oldhamite from the Kaidun carbonaceous chondrite: Relatives of aubrites and EH chondrites? *Meteoritics & Planetary Science* 39:53–60.

Lipschutz M. E., Gaffey M. J., and Pellas P. 1989. Meteoritic parent bodies: Nature, number, size and relation to present-day asteroids. In *Asteroids II*, edited by Binzel R. P., Gehrels T., and Matthews M. S. Tucson, AZ: The University of Arizona Press. pp. 740–777.

MacPherson G. J., Jarosewich E., and Lowenstein P. 1993. Magombedze: A new H-chondrite with light-dark structure. *Meteoritics* 28:138–142.

Mason B. 1979. Cosmochemistry, part 1. Meteorites. In *Data of geochemistry*, 6th ed., edited by Fleischer M. Geological Survey Professional Paper 440-B-1. Washington, D. C.: U.S. Geological Survey. pp. B1–B132.

Meibom A. and Clark B. E. 1999. Evidence for the insignificance of ordinary chondrite material in the asteroid belt. *Meteoritics & Planetary Science* 34:7–24.

Mikouchi T., Makishima J., Koizumi E., and Zolensky M. E. 2005. Porphyritic olivine-pyroxene clast in Kaidun: First discovery of an ordinary chondrite clast? (abstract #1956). 36th Lunar and Planetary Science Conference. CD-ROM.

Mittlefehldt D. W. 1994. The genesis of diogenites and HED parent body petrogenesis. *Geochimica et Cosmochimica Acta* 58:1537–1552.

Mittlefehldt D. W. and Lindstrom M. M. 1988. Geochemistry of diverse lithologies in antarctic eucrites (abstract). 19th Lunar and Planetary Science Conference. pp. 790–791.

Mittlefehldt D. W., McCoy T. J., Goodrich C. A., and Kracher A. 1998. Non-chondritic meteorites from asteroidal bodies. In *Planetary materials*, edited by Papike J. J. Reviews in mineralogy, vol. 26. Washington, D.C.: Mineralogical Society of America. pp. 4-01–4-170.

Ott U., Herrmann S., Jenniskens P. M., and Shaddad M. 2010. A noble gas study of two stones from the Almahata Sitta meteorite (abstract #1195). 41st Lunar and Planetary Science Conference. CD-ROM.

Prinz M., Nehru C. E., Weisberg M. K., Delany J. S., Yanai K., and Kojima H. 1984. H-chondritic clasts in a Yamato L6 chondrite: Implications for metamorphism. *Meteoritics* 19:292–293.

Prinz M., Weisberg M. K., Nehru C. E., and Delaney J. S. 1986. North Haig and Nilpena: Paired polymict ureilites with Angra dos Reis-related and other clasts (abstract). 17th Lunar and Planetary Science Conference. pp. 681–682.

Prinz M., Weisberg M. K., Nehru C. E., and Delaney J. S. 1987. EET 83309, a polymict ureilite: Recognition of a new group (abstract). 18th Lunar and Planetary Science Conference. pp. 802–803.

Prinz M., Weisberg M. K., and Nehru C. E. 1988. Feldspathic components in polymict ureilites (abstract). 19th Lunar and Planetary Science Conference. pp. 947–948.

Pun A., Keil K., Taylor G. J., and Wieler R. 1998. The Kapoeta howardite: Implications for the regolith evolution of the howardite-eucrite-diogenite parent body. *Meteoritics & Planetary Science* 33:835–851.

Reid A. M., Buchanan P., Zolensky M. E., and Barrett R. A. 1990. The Bholghati howardite: Petrography and mineral chemistry. *Geochimica et Cosmochimica Acta* 54:2161–2166.

Ross A. J., Downes H., Smith C. S., and Jones A. P. 2010. DaG 1047: A polymict ureilite containing exotic clasts including a chondrite (abstract #2361). 41st Lunar and Planetary Science Conference. CD-ROM.

Rubin A. E. 1997. The Galim LL/EH polymict breccia: Evidence for impact-induced exchange between reduced and oxidized meteoritic material. *Meteoritics & Planetary Science* 32:489–492.

Rubin A. E. and Bottke W. F. 2009. On the origin of shocked and unshocked CM clasts in H-chondrite regolith breccias. *Meteoritics & Planetary Science* 44:701–724.

Rubin A. E., Scott E. R. D., Taylor G. J., Keil K., Allen J. S. B., Mayeda T. K., Clayton R. N., and Bogard D. D. 1983. Nature of the H chondrite parent body regolith: Evidence from the Dimmitt breccia. Proceedings, 13th Lunar and Planetary Science Conference. pp. A741–A754.

Rubin A. E., Scott E. R. D., and Keil K. 1997. Shock metamorphism of enstatite chondrites. *Geochimica et Cosmochimica Acta* 61:847–858.

Schulze H., Bischoff A., Palme H., Spettel B., Dreibus G., and Otto J. 1994. Mineralogy and chemistry of Rumuruti: The first meteorite fall of the new R chondrite group. *Meteoritics* 29:275–286.

Scott E. R. D. 2002. Meteorite evidence for the accretion and collisional evolution of asteroids. In *Asteroids III*, edited by Bottke W. F., Cellino A., Paolicchi P. and Binzel R. P. Tucson, AZ: The University of Arizona Press. pp. 697–709.

Scott E. R. D. and Wilson L. 2005. Meteoritic and other constraints on the internal structure and impact history of small asteroids. *Icarus* 74:46–63.

Scott E. R. D., Taylor G. J., and Keil K. 1993. Origin of ureilite meteorites and implications for planetary accretion. *Geophysical Research Letters* 20:415–418.

Sears D. W., Kallemeyn G. W., and Wasson J. T. 1982. The compositional classification of chondrites: II. The enstatite chondrites groups. *Geochimica et Cosmochimica Acta* 46:597–608.

Shedlovsky J. P., Cressy P. J. Jr., and Kohman T. P. 1967. Cosmogenic radioactivities in the Peace River and Harleton chondrites. *Journal of Geophysical Research* 72:5051–5058.

Singletary S. J. and Grove T. L. 2003. Early petrologic processes on the ureilite parent body. *Meteoritics & Planetary Science* 38:95–108.

Sokol A. K. and Bischoff A. 2006. Simultaneous accretion of differentiated or metamorphosed asteroidal clasts and chondrules (abstract). *Meteoritics & Planetary Science* 41:A164.

Sokol A. K., Bischoff A., Marhas K. K., Mezger K., and Zinner E. 2007a. Simultaneous accretion of differentiated or metamorphosed asteroidal clasts and chondrules (abstract). *Meteoritics & Planetary Science* 42:A143.

Sokol A. K., Bischoff A., Marhas K. K., Mezger K., and Zinner E. 2007b. Late accretion and lithification of chondritic parent bodies: Mg isotope studies on fragments from primitive chondrites and chondritic breccias. *Meteoritics & Planetary Science* 42:1291–1308.

Stöffler D., Bischoff A., Buchwald V., and Rubin A. E. 1988. Shock effects in meteorites. In *Meteorites and the early solar system*, edited by Kerridge J. F. and Matthews M. S. Tucson, AZ: The University of Arizona Press. pp. 165–202.

Stöffler D., Keil K., and Scott E. R. D. 1991. Shock metamorphism of ordinary chondrites. *Geochimica et Cosmochimica Acta* 55:3845–3867.

Takeda H. 1987. A coexisting orthopyroxene-pigeonite pair in Yamato 791538 and formation condition of ureilites. *Meteoritics* 22:511–512.

Terada K. and Bischoff A. 2009. Asteroidal granite-like magmatism 4.53 Gyr ago. *The Astrophysical Journal* 699:L68–L71.

Walker D. and Grove T. 1993. Ureilite smelting. *Meteoritics* 28:629–636.

Warren P. H. 2010. Asteroidal depth-pressure relationships and the style of the ureilite anatexis (abstract). *Meteoritics & Planetary Science* 45:A120.

Warren P. H. and Huber H. 2006. Ureilite petrogenesis: A limited role for smelting during anatexis and catastrophic disruption. *Meteoritics & Planetary Science* 41:835–849.

Warren P. H. and Kallemeyn G. W. 1992. Explosive volcanism and the graphite oxygen fugacity buffer on the parent asteroid(s) of the ureilite meteorites. *Icarus* 100:110–126.

Warren P. H. and Rubin A. E. 2006. Melted-reduced pigeonite, vermicular silica, Si-rich glasses, and other impact-smelting products in the LAR 04315 ureilite (abstract). *Meteoritics & Planetary Science* 41:A184.

Wasson J. T. and Kallemeyn G. W. 1988. Compositions of chondrites. *Philosophical Transactions of the Royal Society of London Series A* 325:535–545.

Wasson J. T., Chou C. L., Bild R. W., and Baedecker P. A. 1976. Classification of and elemental fractionation among ureilites. *Geochimica et Cosmochimica Acta* 40:1449–1458.

Weber I., Bischoff A., and Weber D. 2003. TEM investigations on the monomict ureilites Jalanash and Hammadah al Hamra 064. *Meteoritics & Planetary Science* 38:145–156.

Wieler R., Graf T., Pedroni A., Signer P., Pellas P., Fieni C., Suter M., Vogt S., Clayton R. N., and Laul J. C. 1989. Exposure history of the regolithic chondrite Fayetteville: II. Solar-gas-free light inclusions. *Geochimica et Cosmochimica Acta* 53:1449–1459.

Wilkening L. L. 1973. Foreign inclusions in stony meteorites—I. Carbonaceous chondritic xenoliths in the Kapoeta howardite. *Geochimica et Cosmochimica Acta* 37:1985–1989.

Wilson L., Goodrich C. A., and Van Orman J. 2008. Thermal evolution and physics of melt extraction on the ureilite parent body. *Geochimica et Cosmochimica Acta* 72:6154–6176.

Wlotzka F. 1993. A weathering scale for ordinary chondrites (abstract). *Meteoritics* 28:460.

Zolensky M. E. and Ivanov A. 2003. The Kaidun microbreccia meteorite: A harvest from the inner and outer asteroid belt. *Chemie der Erde—Geochemistry* 63:185–246.

Zolensky M. E., Hewins R. H., Mittlefehldt D. W., Lindstrom M. M., Xiao X., and Lipschutz M. E. 1992. Mineralogy, petrology and geochemistry of carbonaceous chondritic clasts in the LEW 85300 polymict eucrite. *Meteoritics* 27:596–604.

Zolensky M. E., Weisberg M. K., Buchanan P. C., and Mittlefehldt D. W. 1996. Mineralogy of carbonaceous chondrite clasts in HED achondrites and the moon. *Meteoritics & Planetary Science* 31:518–537.

Zolensky M. E., Herrin J., Jenniskens P., Friedrich J. M., Rumble D., Steele A., Sandford S. A., Shaddad M. H., Le L., Robinson G. A., and Morris R. V. 2009. Mineralogy of the Almahata Sitta ureilite (abstract). *Meteoritics & Planetary Science* 44:A227.